Scientific Research Publishing

Sedimentary Environment of the Early Ordovician in Danzhai, Guizhou

Yu Pei[1], Youbin He[1], Jinxiong Luo[1], Yantao Zeng[2], Zhan Wen[3]

[1]School of Geosciences, Yangtze University, Wuhan, China
[2]School of Earth Environment and Water Resources, Wuhan, China
[3]Beizhong Work Zone of Hailaer Command Post, Daqing Oil Field, Hulun Buir, China
Email: peiyu920621@163.com

Abstract

This study analyzes the variations in trace element contents and ratios, the distribution patterns of rare earth elements, and the sedimentary environment and its evolution in the Early Ordovician. In particular, the analysis is based on measured section of the Qingjiang Village located in Nangao Town, Danzhai County, Guizhou Province. The analysis also considers thin sections and the characteristics of C, O isotopes. The lower part of the Tongzi Formation has a simple lithology and mainly consists of light gray to gray thin-medium bedded muddy dolomite and dolomicrite with a few dolarenites and dolorudites. The upper part of this formation includes gray thin-medium bedded fine crystalline dolomite and gray massive bioclastic limestone. Only a fraction of gray massive fine crystalline limestone, sparry calcarenite, and calcirudite are on top of the upper part. The Honghuayuan Formation is generally composed of light gray to gray medium-thick bedded or massive bioclastic limestone, reef limestone, and calcarenite with a few sandstones at the bottom. The $\delta^{18}O_{PDB}$ values of 18 samples are less than $-11‰$; in addition, the Pr/Pr* and Ce/Ce* ratios are greater and less than 1, respectively. These data reflect a sedimentary environment. The lower part of the Tongzi Formation might have been formed in an evaporite platform, which was then transformed into a restricted one, which featured a dry climate, a shallow water depth, and an insufficient amount of oxygen. By contrast, the upper part of the formation was deposited in an open platform, which featured a humid climate and relatively increased water depth and reducibility. During the sedimentary period of the Honghuayuan Formation, the water energy further increased, the climate became humid, the water depth increased, and the reducibility increased. Correspondingly, the sedimentary environment, which originally comprised littoral facies that slowly developed into an open platform and into a platform marginal bank, gradually evolved into a platform

marginal reef.

1. Introduction

The Early Ordovician section in the Qingjiang Village of Nangao Town in Danzhai County, Guizhou Province shows clear stratigraphic boundaries ([Figure 1](#)), complete layers, reliable depositional marks, and abundant fossils. This section is an excellent carrier of the sedimentary environment evolution in southeast Guizhou and partially reflects the Early Ordovician tectonic evolution of South China. During the Palaeozoic Era, southeast Guizhou and its peripheral areas indicated a strong potential for hydrocarbon [1]-[9]. As an important marine stratum, the Lower Ordovician features desirable reservoir properties. In the section under study, the outcrop fractures and dissolved pores are filled with bitumen. To gain further insights into reservoir development characteristics and strengthen petroleum geology research by exploring the basic issues related to reservoir formation and the potential of marine oil and gas exploration in the south, we must clarify the characteristics and evolution of the sedimentary environment. Biostratigraphy researches, such as trilobites, corals, conodonts and so on, are conducted in the Early Ordovician of Guizhou Province [10] [11] [12] [13] [14]. The paleogeography of Tongzi Formation and Huanghuayuan Formatin is also reconstructed in Guizhou Province [15] [16]. Little research on paleoenvironment by applying trace elements is done. Therefore, this study discusses the Early Ordovician paleoenvironment, including paleoclimate, paleosalinity, paleowater depth, paleoxygenation facies, and its evolution in the Danzhai region of Guizhou on the basis of petrology characteristics and by synthetically using C, O isotopes and trace elements.

2. Regional Geological Conditions

The Early Ordovician in South China belongs to the passive continental margin stage. A suit of giant carbonate rock wedge develops along the continental margin [17] [18] [19] [20]. The Lower Ordovician vertically displays an upward-deepening transgressive sequence. Danzhai, Guizhou lies in the upper Yangtze region on the border between the Qiannan Depression and the Jiangnan Uplift ("Qian" is the shortened term for Guizhou Province). The Lower Ordovician is well exposed and can be divided into the Tongzi and Honghuayuan Formations in the vertical context [21] ([Figure 2](#)). This part is in conformable contact with the underlying Loushanguan Formation, which belongs to the Upper Cambrian, and with the overlying Dawan Formation, which belongs to the Middle Ordovician ([Figure 2](#)).
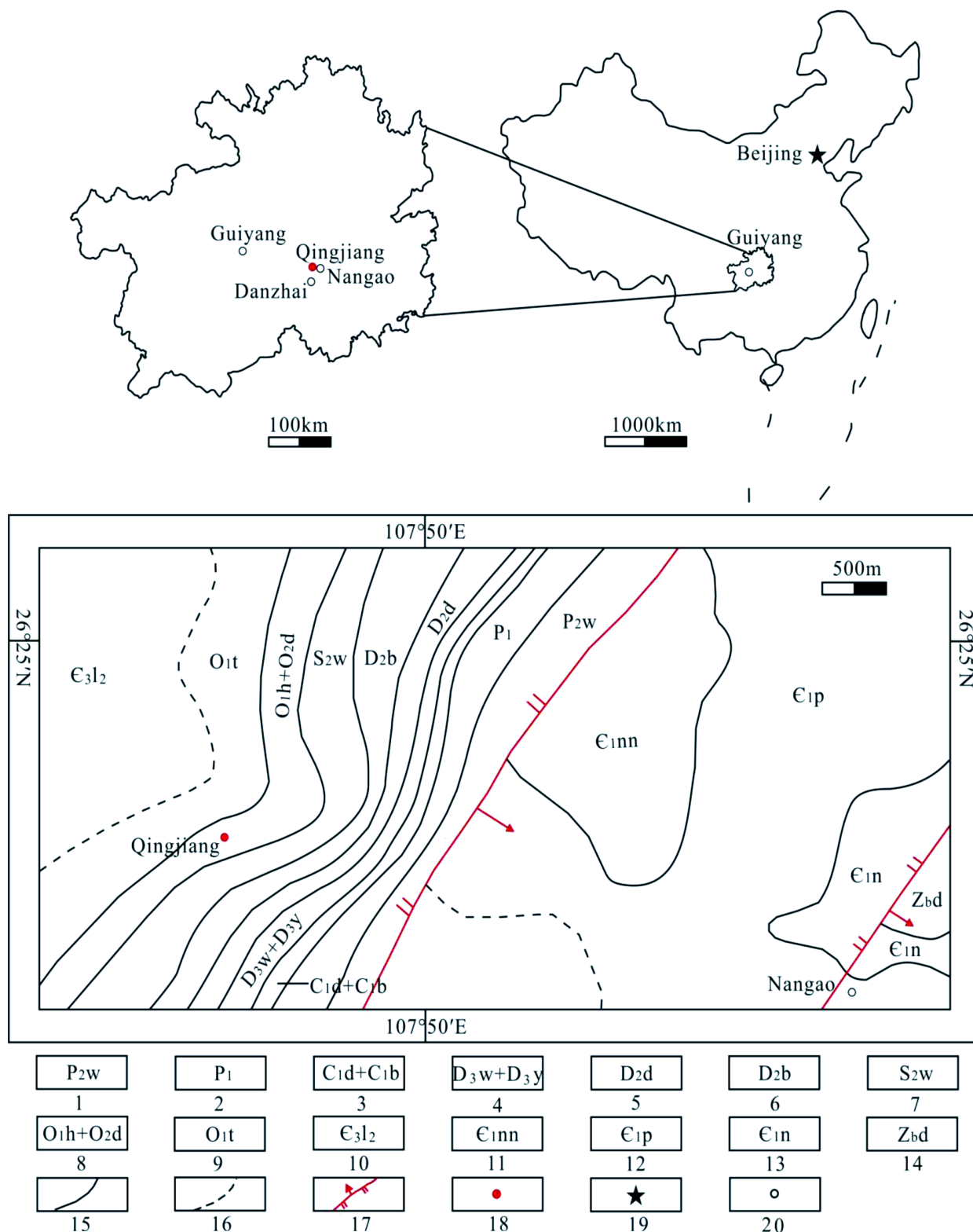
Figure 1. Geological map of Nangao that shows the location of the study section [22]; *Note: Fm. stands for formation; 1, Wujiaping Fm.; 2, Liangshan Fm., Qixia Fm., Maokou Fm.; 3, Datang Stage, Baizuo Fm.; 4, Wangchengpo Fm., Yaosuo Fm.; 5, Dushan Fm.; 6, Shangbangzhai Fm.; 7, Wengxiang Fm.; 8, Honghuayuan Fm., Dawan Fm.; 9, Tongzi Fm.; 10, Second Member, Lushan Fm.; 11, Nangao Fm.; 12, Palang Fm.; 13, Niutitang Fm.; 14, Dengying Fm.; 15, Stratigraphic boundary; 16, Speculative stratigraphic boundary; 17, Reversed fault; 18, Study section; 19, Capital; 20, City.

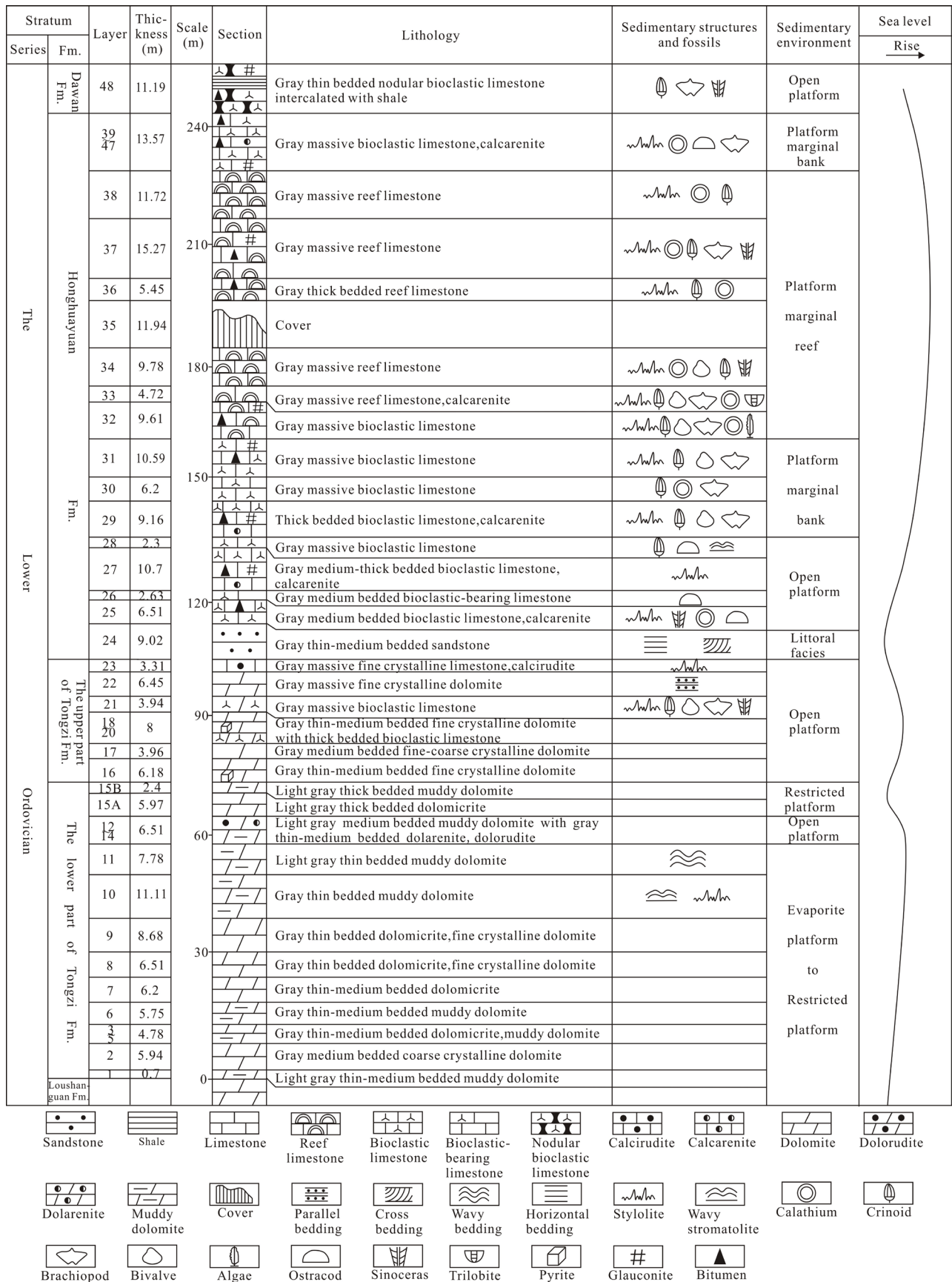| Stratum — Series	Stratum — Fm.	Layer	Thickness (m)	Scale (m)	Section	Lithology	Sedimentary structures and fossils	Sedimentary environment	Sea level Rise
The Lower Ordovician	Dawan Fm.	48	11.19	240		Gray thin bedded nodular bioclastic limestone intercalated with shale		Open platform	
	Honghuayuan Fm.	39–47	13.57			Gray massive bioclastic limestone, calcarenite		Platform marginal bank	
		38	11.72			Gray massive reef limestone			
		37	15.27	210		Gray massive reef limestone			
		36	5.45			Gray thick bedded reef limestone		Platform marginal reef	
		35	11.94			Cover			
		34	9.78	180		Gray massive reef limestone			
		33	4.72			Gray massive reef limestone, calcarenite			
		32	9.61			Gray massive bioclastic limestone			
		31	10.59	150		Gray massive bioclastic limestone		Platform marginal bank	
		30	6.2			Gray massive bioclastic limestone			
		29	9.16			Thick bedded bioclastic limestone, calcarenite			
		28	2.3			Gray massive bioclastic limestone		Open platform	
		27	10.7			Gray medium-thick bedded bioclastic limestone, calcarenite			
		26	2.63	120		Gray medium bedded bioclastic-bearing limestone			
		25	6.51			Gray medium bedded bioclastic limestone, calcarenite			
		24	9.02			Gray thin-medium bedded sandstone		Littoral facies	
	The upper part of Tongzi Fm.	23	3.31			Gray massive fine crystalline limestone, calcirudite			
		22	6.45			Gray massive fine crystalline dolomite			
		21	3.94	90		Gray massive bioclastic limestone		Open platform	
		18–20	8			Gray thin-medium bedded fine crystalline dolomite with thick bedded bioclastic limestone			
		17	3.96			Gray medium bedded fine-coarse crystalline dolomite			
		16	6.18			Gray thin-medium bedded fine crystalline dolomite			
	The lower part of Tongzi Fm.	15B	2.4			Light gray thick bedded muddy dolomite		Restricted platform	
		15A	5.97			Light gray thick bedded dolomicrite			
		12–14	6.51	60		Light gray medium bedded muddy dolomite with gray thin-medium bedded dolarenite, dolorudite		Open platform	
		11	7.78			Light gray thin bedded muddy dolomite			
		10	11.11			Gray thin bedded muddy dolomite		Evaporite platform to Restricted platform	
		9	8.68	30		Gray thin bedded dolomicrite, fine crystalline dolomite			
		8	6.51			Gray thin bedded dolomicrite, fine crystalline dolomite			
		7	6.2			Gray thin-medium bedded dolomicrite			
		6	5.75			Gray thin-medium bedded muddy dolomite			
		3–5	4.78			Gray thin-medium bedded dolomicrite, muddy dolomite			
		2	5.94			Gray medium bedded coarse crystalline dolomite			
		1	0.7	0		Light gray thin-medium bedded muddy dolomite			
	Loushanguan Fm.								

Legend:

Sandstone · Shale · Limestone · Reef limestone · Bioclastic limestone · Bioclastic-bearing limestone · Nodular bioclastic limestone · Calcirudite · Calcarenite · Dolomite · Dolorudite

Dolarenite · Muddy dolomite · Cover · Parallel bedding · Cross bedding · Wavy bedding · Horizontal bedding · Stylolite · Wavy stromatolite · Calathium · Crinoid

Brachiopod · Bivalve · Algae · Ostracod · Sinoceras · Trilobite · Pyrite · Glauconite · Bitumen

Figure 2. Columnar section of the Lower Ordovician rock characteristics and sedimentary environment in Danzhai, Guizhou.

3. Sample Collection, Test, and Data Validity Analysis

The Lower Ordovician section in the Qingjiang Village of Nangao Town in Danzhai County is geographically located at 26˚24'21" north latitude and 107˚48'55.3" east longitude and has a thickness of 267.53 m. Field survey indicates that the Tongzi Formation is mainly composed of light gray to gray thin-medium bedded muddy dolomite, dolomicrite, fine crystalline dolomite, and massive bioclastic limestone; it is divided into 23 layers (Figure 2). The Honghuayuan Formation principally includes light gray to gray medium-thick bedded or massive bioclastic limestone, reef limestone, and calcarenite with a few sandstones at the bottom; it is divided into 24 layers (Figure 2). In this study, 10 samples are collected from the Tongzi Formation, and another 10 samples are collected from the Honghuayuan Formation. The thin sections of the samples are ground, and the carbon and oxygen isotopes and trace elements are determined (Table 1). These geochemical samples are processed and tested with an ELEMENT XR plasma mass spectrum analyzer in a test research center at the Nuclear Industry Geological Institute, Beijing.

The contents of isotopes and trace elements are related to the sedimentary environment, lithology, terrigenous clastic content, and diagenesis [23]. The chemical compositions of carbonate rocks are influenced by diagenesis when their $\delta^{18}O_{PDB}$ values are less than −11‰ [24]. Derry *et al.* [25] argue that dolomitization is not a precondition of carbonate rocks that are unaffected by diagenesis. The $\delta^{13}C$ values of carbonate rocks represent carbon isotope contents at the Proto-Oceanic level when their $\delta^{18}O_{PDB}$ values are more than −10‰ [26]. These carbon isotope contents are associated with sea level changes and vary between −5‰ and 5‰.

The rock samples in this study are mainly gray thin-medium bedded muddy dolomite and dolomicrite and light gray to gray massive bioclastic and reef limestones. The Pr/Pr* ratios of the Lower Ordovician samples are greater than 1, whereas the Ce/Ce* ratios are less than 1. As such, the influence of terrigenous clasts on the research samples is ruled out. The samples have positive and negative $\delta^{13}C_{PDB}$ values, most of which are negative and range from −1.60‰ to 0.50‰. The negative $\delta^{18}O_{PDB}$ values of the samples only vary between −9.00‰ and −2.00‰. This observation indicates that the carbonate rocks may have undergone burial diagenesis (Figure 3) and not dolomization. To reflect the sedimentary
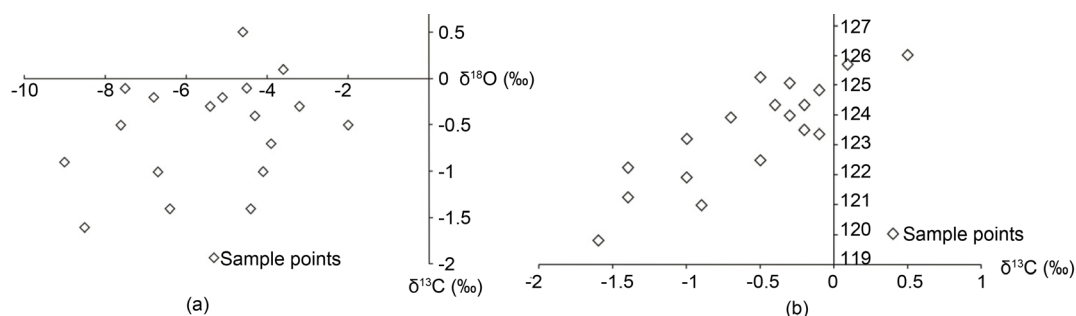

Figure 3. (a) Carbonate rock C, O isotope distribution chart of the lower ordovician; (b) carbonate rock $\delta^{13}C$, Z distribution chart of the lower ordovician.

Table 1. Carbon and oxygen isotopes and trace element contents of carbonate rocks in the lower ordovician.

Sample number	Rock type	C ‰	O ‰	B µg/g	Cu µg/g	Ga µg/g	Sr µg/g	Ba µg/g	V µg/g	Ni µg/g	Cr µg/g	U µg/g	Th µg/g	Co µg/g	La µg/g	Ce µg/g	Pr µg/g	Nd µg/g	Sm µg/g	Eu µg/g	Gd µg/g	Tb µg/g	Dy µg/g	Ho µg/g	Er µg/g	Tm µg/g	Yb µg/g	Lu µg/g
Qing-1	Muddy dolomite	−0.7	−3.9	24.20	20.4	3.91	49.1	45.0	20.00	4.45	16.50	1.160	2.490	4.03	7.33	13.10	1.57	5.86	1.160	0.225	1.100	0.174	0.905	0.176	0.541	0.078	0.467	0.068
Qing-3		0.5	−4.6	35.20	27.5	4.23	84.6	44.6	20.10	9.69	17.80	0.773	1.890	6.78	6.19	10.90	1.30	4.57	0.920	0.196	0.890	0.138	0.764	0.156	0.453	0.070	0.412	0.057
Qing-2	Dolomicrite	−0.1	−4.5	3.44	160.0	0.48	44.8	6.1	2.68	1.01	1.93	0.261	0.294	3.26	1.01	1.96	0.25	0.89	0.181	0.041	0.181	0.027	0.163	0.036	0.098	0.016	0.108	0.014
Qing-5		−1.4	−6.4	6.59	24.4	0.33	45.7	11.4	3.61	1.15	1.62	0.462	0.257	3.48	1.61	3.25	0.36	1.31	0.236	0.053	0.266	0.039	0.206	0.041	0.127	0.017	0.103	0.015
Qing-4	Dolorudite	−1.4	−4.4	21.80	25.0	2.13	61.4	163.0	8.05	3.82	7.49	0.773	1.160	3.81	3.72	7.75	0.89	3.16	0.655	0.139	0.628	0.101	0.568	0.122	0.348	0.056	0.326	0.049
Qing-6		−1.5	−12.8	9.84	8.2	0.98	58.4	12.0	10.10	2.78	4.30	0.760	0.651	4.44	3.88	8.09	0.83	3.06	0.601	0.134	0.606	0.089	0.540	0.099	0.291	0.043	0.271	0.034
Qing-7	Fine crystalline dolomite	−0.1	−7.5	21.90	14.9	2.21	321.0	180.0	8.10	5.58	8.40	0.549	1.420	7.11	6.75	12.00	1.43	5.01	0.967	0.202	0.980	0.147	0.831	0.172	0.509	0.075	0.460	0.063
Qing-9		−1.0	−6.7	23.30	44.9	2.37	60.3	41.7	10.90	2.21	7.41	1.190	2.870	3.94	5.84	13.10	1.52	5.52	1.170	0.226	1.090	0.180	1.050	0.223	0.651	0.105	0.637	0.091
Qing-10	Calcirudite	−1.6	−8.5	6.01	5.5	0.56	239.0	99.3	2.82	1.90	2.23	1.630	0.557	5.01	4.40	7.71	0.89	3.19	0.637	0.135	0.648	0.100	0.534	0.107	0.314	0.046	0.267	0.038
Qing-12	Limestone	−0.2	−6.8	5.11	9.4	0.78	341.0	21.3	2.85	2.69	2.63	0.645	0.674	5.33	3.83	7.10	0.80	2.92	0.619	0.136	0.619	0.099	0.585	0.126	0.352	0.053	0.342	0.046
Qing-15		−0.3	−5.4	12.20	11.4	1.32	273.0	148.0	4.55	3.83	4.43	0.607	1.150	5.82	4.80	9.18	1.04	3.72	0.774	0.161	0.769	0.121	0.700	0.144	0.409	0.066	0.381	0.054
Qing-16	Reef limestone	−0.5	−7.6	4.14	47.5	0.74	183.0	34.8	8.73	2.56	2.39	1.540	0.770	4.41	5.44	10.40	1.22	4.76	1.080	0.225	1.080	0.173	1.000	0.213	0.591	0.089	0.521	0.070
Qing-17		−0.3	−3.2	8.84	27.9	1.20	307.0	174.0	4.16	2.70	4.15	0.710	0.984	4.06	5.59	10.60	1.19	4.43	0.957	0.195	0.926	0.149	0.866	0.174	0.494	0.076	0.442	0.061
Qing-8		−0.5	−2.0	6.14	31.4	0.62	187.0	10.9	4.42	1.94	2.27	0.811	0.424	4.07	2.25	4.12	0.46	1.57	0.332	0.068	0.344	0.051	0.277	0.059	0.169	0.026	0.152	0.022
Qing-11		−.9	−9.0	13.60	34.7	1.70	327.0	33.2	5.66	3.65	5.74	0.711	1.160	6.12	5.06	9.53	1.10	3.88	0.774	0.145	0.724	0.112	0.622	0.122	0.358	0.051	0.324	0.045
Qing-13		0.1	−3.6	1.25	8.3	0.18	161.0	14.3	1.25	0.57	0.79	0.340	0.162	4.89	1.70	3.38	0.37	1.41	0.308	0.066	0.329	0.052	0.307	0.064	0.184	0.029	0.176	0.024
Qing-14	Bioclastic limestone	−0.3	−15.1	7.11	28.8	0.45	209.0	25.8	1.90	0.82	1.18	0.437	0.381	4.49	3.86	8.04	0.90	3.44	0.777	0.173	0.771	0.128	0.733	0.158	0.442	0.066	0.390	0.054
Qing-16		−0.5	−7.6	4.14	47.5	0.74	183.0	34.8	8.73	2.56	2.39	1.540	0.770	4.41	5.44	10.40	1.22	4.76	1.080	0.225	1.080	0.173	1.000	0.213	0.591	0.089	0.521	0.070
Qing-18		−1.0	−4.1	13.30	18.6	1.50	66.0	20.8	7.40	1.97	4.70	0.592	1.160	3.80	7.24	15.10	1.75	6.20	1.210	0.253	1.150	0.178	0.985	0.201	0.578	0.087	0.508	0.069
Qing-19		−0.4	−4.3	3.90	14.5	0.60	272.0	389.0	3.68	1.51	1.59	0.813	0.587	5.05	3.30	6.88	0.74	2.83	0.632	0.171	0.651	0.102	0.583	0.122	0.342	0.051	0.325	0.047
Qing-20		−0.2	−5.1	13.30	14.6	1.36	263.0	184.0	4.75	2.99	4.35	0.681	1.220	6.05	6.25	12.60	1.33	4.92	1.040	0.228	1.040	0.168	0.983	0.208	0.614	0.096	0.586	0.081

environment characteristics, the values of samples Qing-6 and Qing-14 are disregarded because their $\delta^{18}O_{PDB}$ values are −12.8 and −15.1, respectively. The effect of terrigenous source on Eu being eliminated indicates that such variable is influenced by seawater. Consequently, no correlation is observed between Ce/Ce* and Eu/Eu*. This finding implies that diagenesis only slightly influences Eu anomaly, which, in turn, represents the original condition of seawater. The remaining 18 samples are used to analyze the ancient environment.

4. Petrologic Characteristics

The lower part of the Tongzi Formation of the Qingjiang profile has a simple lithology and mainly consists of light gray to gray thin-medium bedded muddy dolomite and dolomicrite (Figure 2, Figure 4(a), and Figure 5(a), Figure 5(b)) with small amounts of dolarenite and dolorudite (Figure 2 and Figure 4(a)). The weathered color of this part is grayish yellow, and it contains various amounts of mud and siliceous concretion, motted pyrite, and calcite veins. The sedimentary structures of this section include wavy bedding, stratiform stromatolite, and stylolite (Figure 2). Fossils are rarely observed (Figure 2), thus indicating that the section primarily consists of penecontemporaneous dolomite. By contrast, the upper part of the Tongzi Formation includes gray thin-medium bedded fine crystalline dolomite (Figure 2 and Figure 5(c)) and gray massive bioclastic limestone. The top part comprises only a few gray massive fine crystalline limestone, sparry calcarenite (Figure 5(d)), and calcirudite. Bioclastics include crinoids, bivalves, brachiopods, and *sinoceras* (Figure 2), which are autochthonous deposits. These characteristics indicate increased water depth and energy.

The Tongzi Formation is conformably overlain by the Honghuayuan Formation. The boundary line between these formations is distinct and consists of gray thin-medium bedded sandstones with a thickness of 9 m (belonging to the Honghuayuan Formation) (Figure 2 and Figure 4(b)). The rock types in the Honghuayuan Formation are mainly light gray to gray medium-thick bedded or massive bioclastic limestone (Figure 2, Figure 4(c), Figure 4(d), and Figure 5(e)), reef limestone (Figure 2, Figure 4(e), and Figure 5(f)), and calcarenite (Figure 2 and Figure 5(g), Figure 5(h)) with a few sandstones at the bottom (Figure 2 and Figure 4(b)). Bioclasts in situ include *calathium*, crinoids, brachiopods, algae, ostracods, trilobites, and so on (Figure 2). Horizontal bedding, low angle cross bedding, and wavy stromatolite can be observed in the Honghuayuan Formation (Figure 2 and Figure 4(f)). These characteristics indicate a further increase in water energy and depth.

5. Distribution Patterns of Rare Earth Elements

The maximum and minimum values of the total rare earth elements (ΣREE) are 35.51 μg/g and 4.97 μg/g, respectively, with a mean of 21.52 μg/g. This mean value is significantly smaller than that of the North American shale (*i.e.*, 173.2 μg/g) in line with the characteristics of the carbonate rocks of low ΣREE. The

light rare earth element (LREE) values of the samples range from 4.33 µg/g to 31.75 µg/g with a mean of 18.99 µg/g. The heavy rare earth element (HREE) values range from 0.64 µg/g to 4.03 µg/g with a mean of 2.53 µg/g. The LREE/HREE ratio
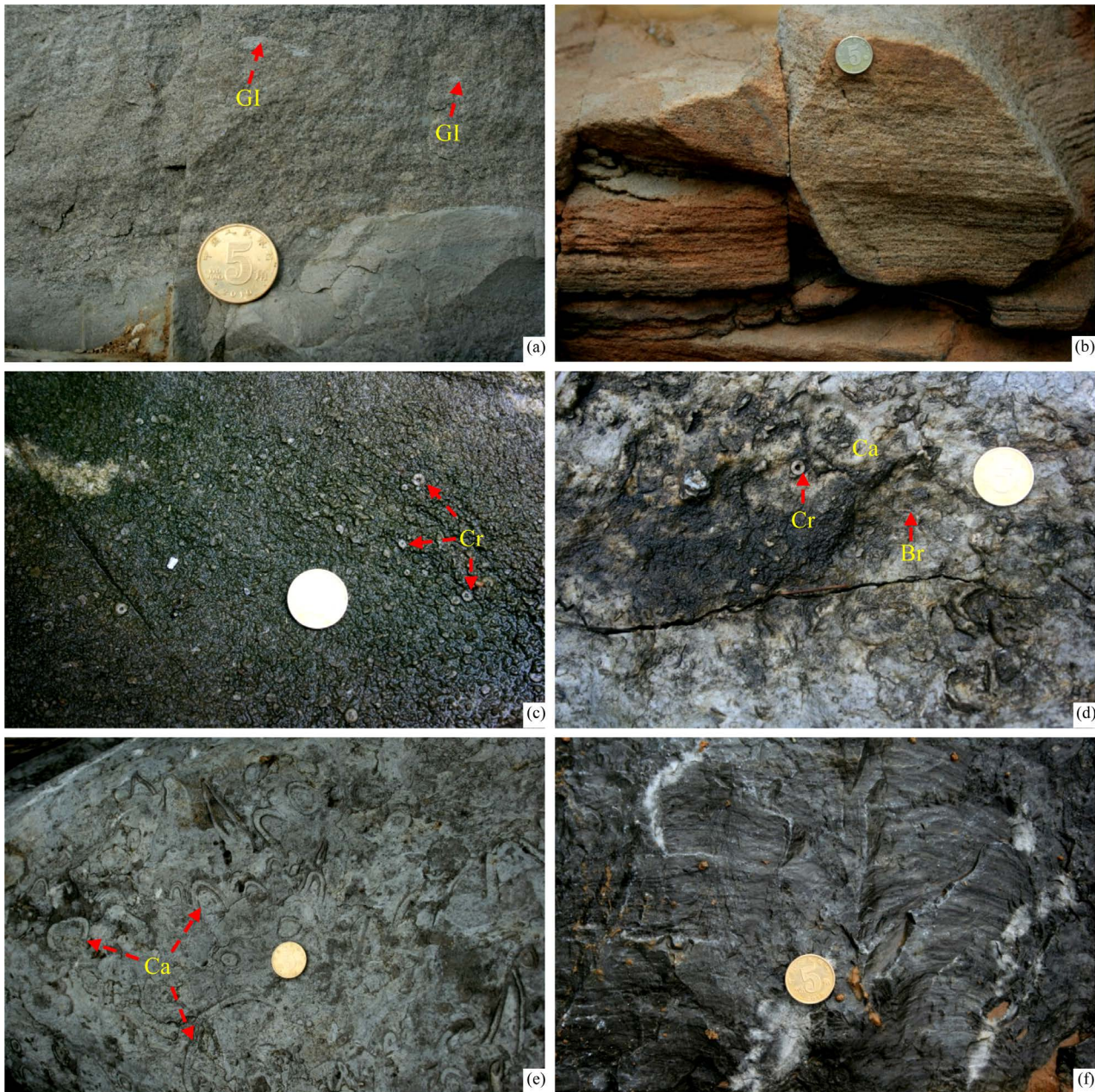

Figure 4. Outcrop photos of the Lower Ordovician. (a) Light gray medium bedded dolomicrite in the lower part, gray thin-medium bedded dolorudite and dolarenite in the upper part, gravel-sized intraclast as large as 15 mm × 5 mm, long strip shape, as small as 2 mm × 2 mm, round or oval, 13th layer, the lower part of the Tongzi Formation; (b) Gray (earthy yellow) thin-medium bedded sandstone with parallel and cross bedding, the boundary line between the Tongzi and Honghuayuan Formations, 24th layer, Honghuayuan Formation; (c) Gray medium-thick bedded bioclastic limestone, high bioclastic content of about 80% and most are crinoids as large as 5 mm × 5 mm and as small as 1 mm × 1 mm, 27th layer, Honghuayuan Formation; (d) Gray massive bioclastic limestone, high bioclastic content of about 80% and most are crinoids, brachiopods, *calathium*, and so on, 30th layer, Honghuayuan Formation; (e) Gray massive reef limestone, high bioclastic content of about 60% and most are *calathium*, 37th layer, Honghuayuan Formation; (f) Wavy stromatolite, gray stromatolite limestone, 28th layer, Honghuayuan Formation; *Note: coin diameter = 2 cm; GI, Cr, Ca, and Br stand for gravel-sized intraclast, crinoid, *calathium*, and brachiopod, respectively.
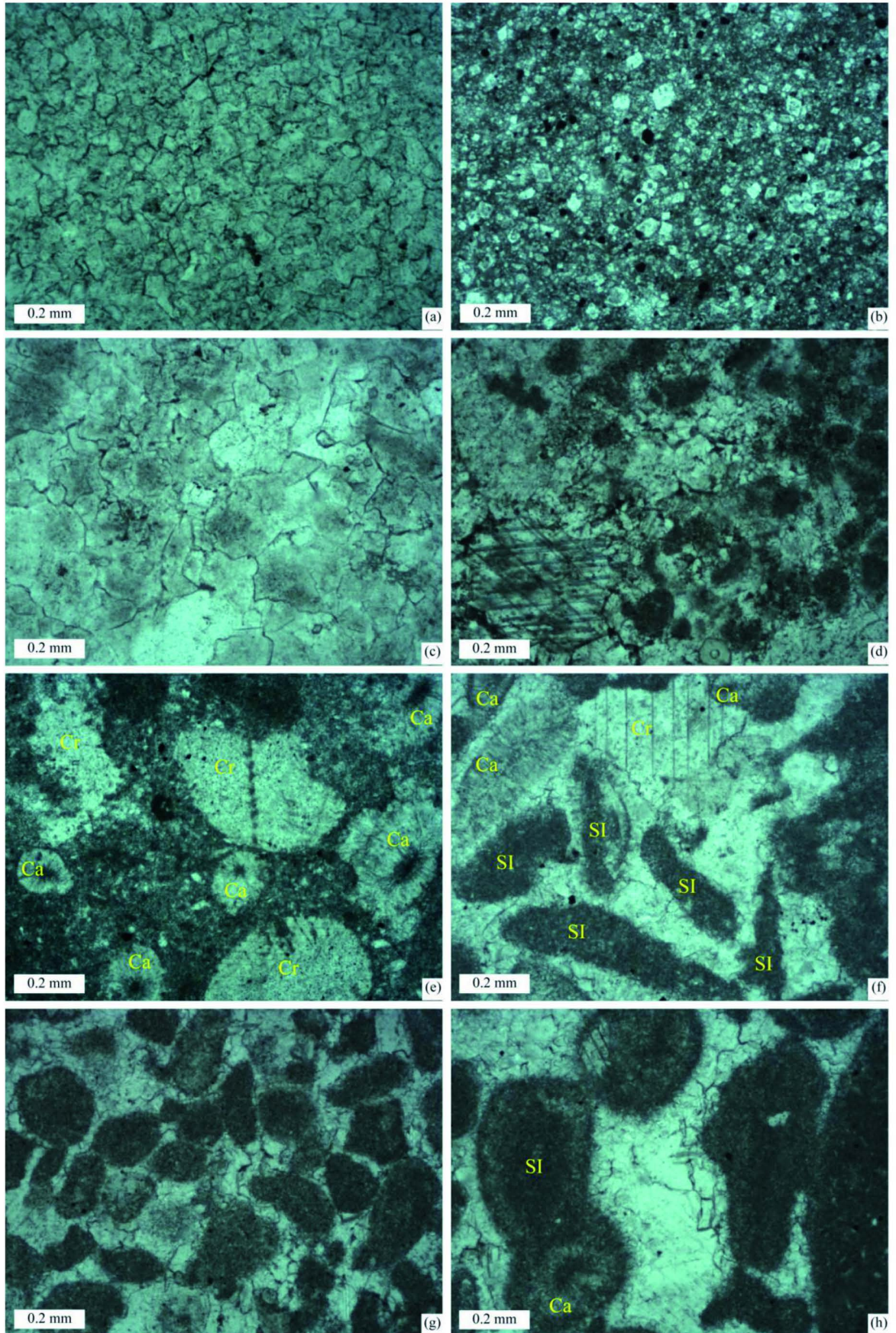
Figure 5. Microscopic photos of the Lower Ordovician. (a) Dolomicrite, subhedral dolomite as large as 0.1 mm × 0.1 mm and as small as 0.02 mm × 0.02 mm, 5th layer, lower part of Tongzi Formation, plane polarized light; (b) Dolomicrite, euhedral dolomite as large as 0.05 mm × 0.05 mm and as small as 0.01 mm × 0.01 mm, 14th layer, lower part of Tongzi Formation, plane polarized light; (c) Fine crystalline dolomite, subhedral dolomites as large as 0.25 mm × 0.25 mm and as small as 0.1 mm × 0.1 mm, 18th layer, upper part of Tongzi Formation, plane polarized light; (d) Sparry calcarenite, sand-sized intraclasts as large as 0.15 mm × 0.15 mm and as small as 0.1 mm × 0.1 mm, good sorting and rounding, 23rd layer, upper part of Tongzi Formation, plane polarized light; (e) Bioclastic limestone cemented by micrite with *calathium*, 30th layer, Honghuayuan Formation, plane polarized light; (f) Reef limestone cemented by sparite with *calathium* and crinoid, 37th layer, Honghuayuan Formation, plane polarized light; (g) Sparry calcarenite, sand-sized intraclasts as large as 0.2 mm × 0.2 mm and as small as 0.1 mm × 0.1 mm, poor sorting and rounding, 25th layer, Honghuayuan Formation, plane polarized light; (h) Sparry calcarenite, sand-sized intraclasts as large as 0.4 mm × 0.4 mm and as small as 0.1 mm × 0.1 mm, poor sorting, good rounding, with *calathium*, 27th layer, Honghuayuan Formation, plane polarized light; *Note: SI, Cr, and Ca denote sand-sized intraclast, crinoid, and *calathium*, respectively.

fluctuates from 6.19 to 8.69 with a mean of 7.49 (**Figure 6**). This ratio is slightly higher than that of the North American shale (*i.e.*, 7.50 μg/g), thus reflecting the enrichment in LREE and loss in HREE.

$(La/Yb)_N$ is the slope of the REE distribution curve standardized by the North American shale, the ratios of which range from 0.89 to 1.60 with a mean of 1.24. This slope depicts the right-dipping curve and the enrichment of LREE. The $(La/Sm)_N$ and $(Gd/Yb)_N$ ratios reflect the degree of fractionation of LREE and HREE, respectively. The $(La/Sm)_N$ ratios range from 0.89 to 1.24 with a mean of 1.08, thus indicating that the LREE fractionation is relatively low. The $(Gd/Yb)_N$ ratios range from 1.00 to 1.54 with a mean of 1.24, thus indicating that the HREE fractionation is relatively low (**Figure 6**) as well. In sum, the ΣREE and HREE contents of the carbonate rock samples are low, whereas the LREE contents are relatively high. The above findings also indicate that the LREE and HREE fractionations are low (**Figure 7**).

6. Sedimentary Environment Analysis

6.1. Paleoclimate

The climate of the Early Ordovician covered by this study was mainly arid, and the degree of drought from the sedimentary period of the Tongzi Formation to that of the Honghuayuan Formation was reduced. These characteristics can be explained as follows. The $\delta^{18}O_{PDB}$ values of the Lower Ordovician vary between −9.00‰ and −2.00‰ with a mean of −5.42‰, thus demonstrating a positive anomaly. The values for the Tongzi Formation range from −8.50‰ to −2.00‰ with a mean of −5.39‰. The values for the Honghuayuan Formation vary between −9.00‰ and −3.20‰ with a mean of −5.46‰. The mobility of ^{16}O is higher than that of ^{18}O. ^{16}O content decreases because of evaporation, thereby relatively increasing ^{18}O content. The Sr/Cu ratios of the Lower Ordovician vary between 0.28 and 43.61 with a mean of 12.60. The ratios for the Tongzi Formation range from 0.28 to 43.61 with a mean of 9.17. The ratios for the Honghuayuan Formation vary between 3.55 and 36.35 with a mean of 16.03 (**Figure 8**). Generally, when Sr/Cu ratios are between 1.3 and 5.0, the climate is humid. By contrast, when these ratios are greater than 5.0, the climate is dry [27]. The

dolomites in the lower part of the Tongzi Formation are inferred to be formed by penesyndiagenesis, and the sedimentary environment might be under the condition of drought. The variations in ^{18}O content and Sr/Cu ratio may reflect a periodic climate change vertically.
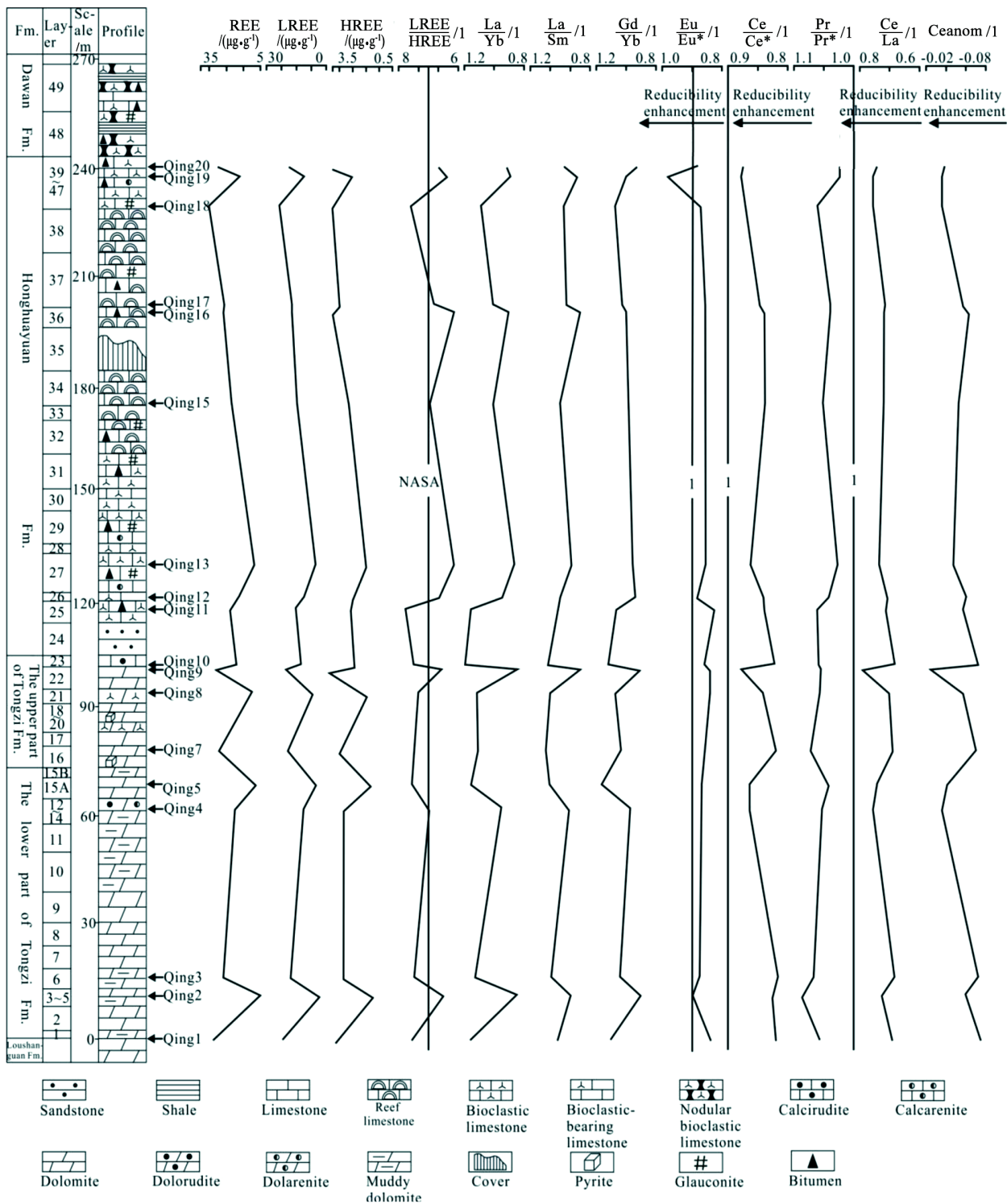

Figure 6. REE contents and paleoenvironmental characteristics of the carbonate rocks in the Lower Ordovician.
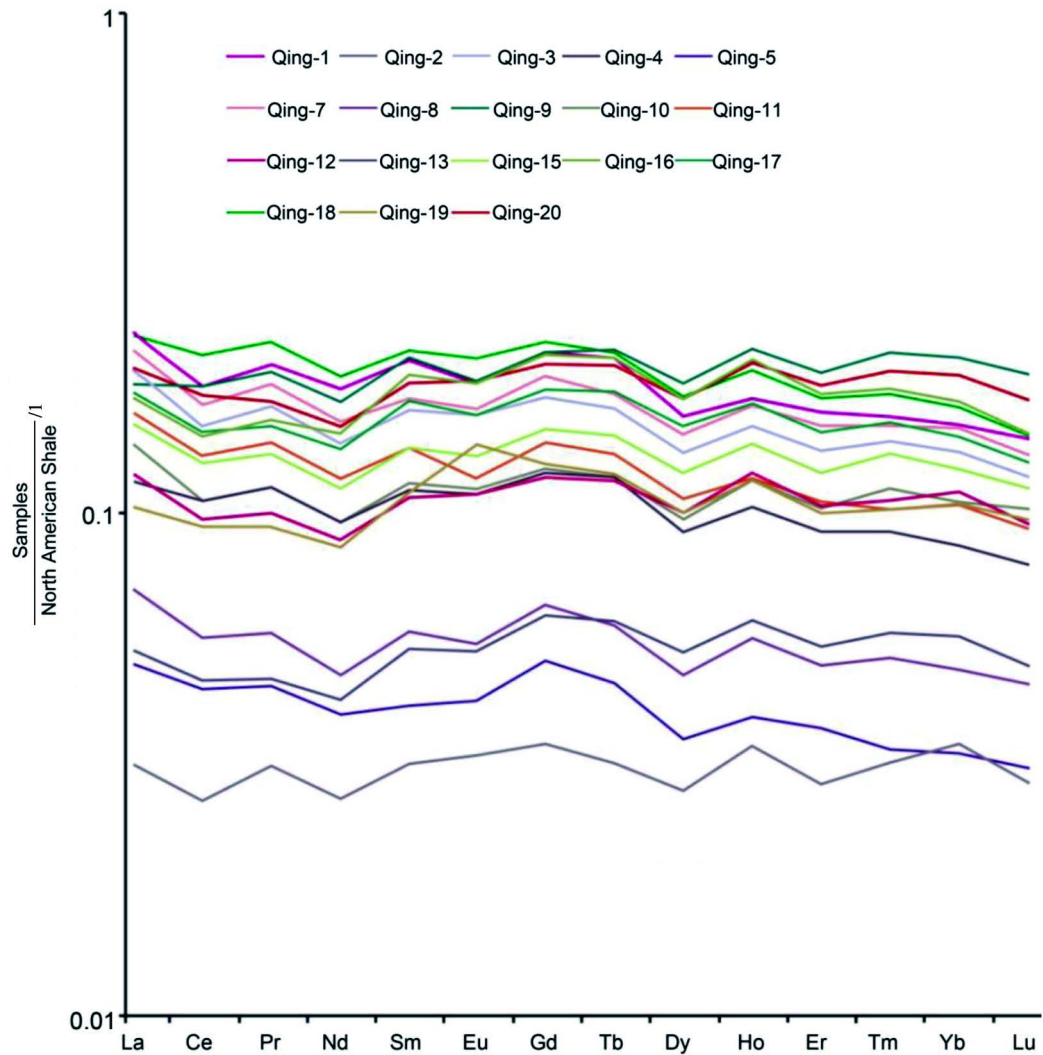
Figure 7. North American shale normalized REE patterns of carbonate rocks in the Lower Ordovician.

6.2. Paleosalinity

The sedimentary environment of the Early Ordovician was generally a marine environment. Moreover, the salinity from the sedimentary period of the Tongzi Formation to that of the Honghuayuan Formation slightly decreased. The samples in this study have positive and negative $\delta^{13}C_{PDB}$ values ranging from $-1.60‰$ to $0.50‰$, but most values are negative; the mean value is $-0.56‰$. By contrast, the $\delta^{18}O_{PDB}$ values of the samples are only negative and vary between $-9.00‰$ and $-2.00‰$ with a mean of $-5.42‰$. The $\delta^{13}C_{PDB}$ and $\delta^{18}O_{PDB}$ values are high. Epstein and Mayeda [28] determine that with an increase in salinity, O^{18}/O^{16} and $^{13}C/^{12}C$ increase. The Z values of all the samples, except for one (*i.e.*, 119.79), are greater than 120. These values vary between 119.79 and 126.03 (Figure 8) with a mean of 123.46, thus indicating a marine environment. The empirical formula proposed by Keith *et al.* [29] is commonly adopted to quantitatively determine the salinity of paleowater.

$$Z = 2.048 \times \left(\delta^{13}C_{PDB} + 50 \right) + 0.498 \times \left(\delta^{18}O_{PDB} + 50 \right)$$
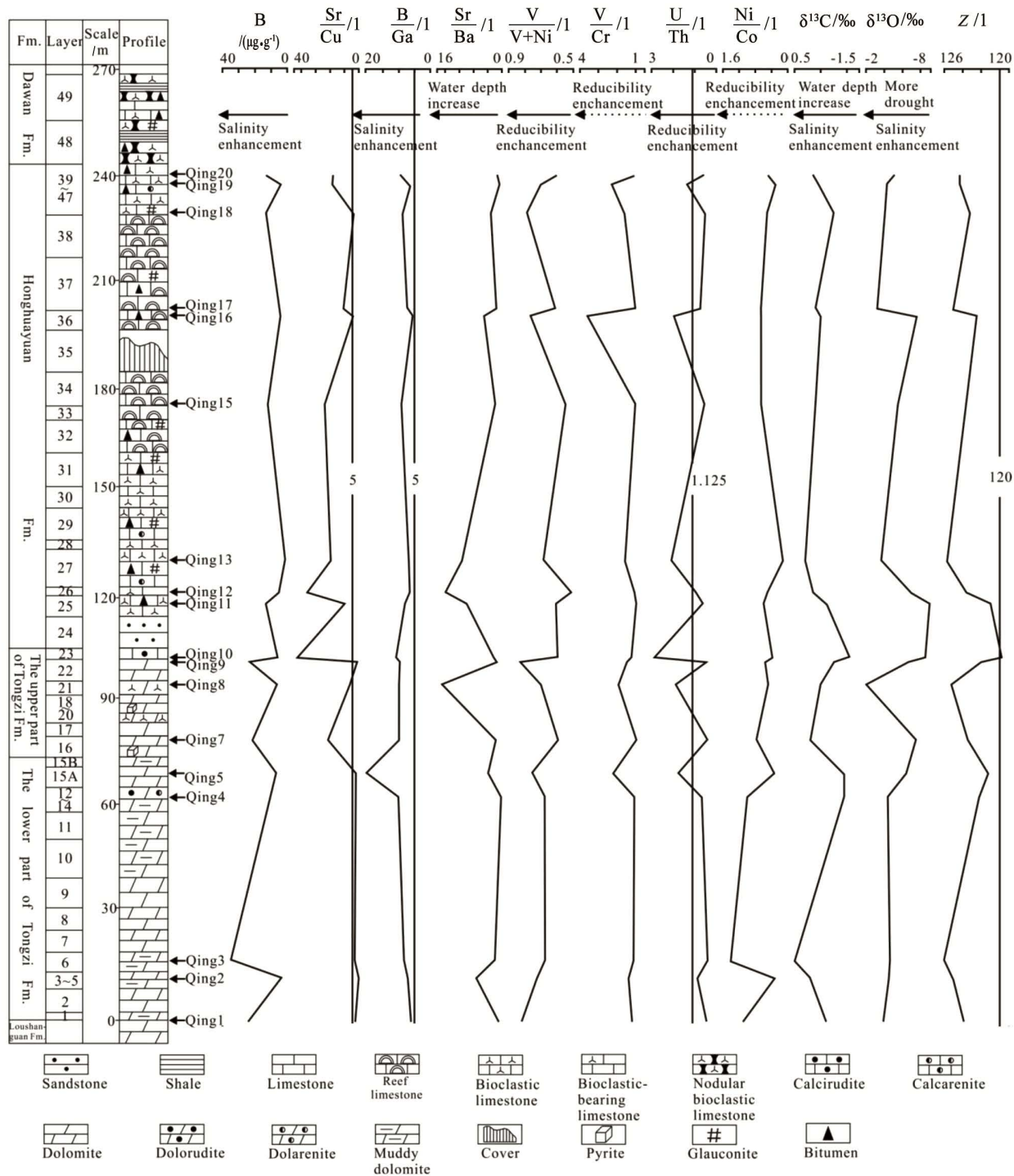
Figure 8. Trace element contents and paleoenvironmental characteristics of the carbonate rocks in the lower ordovician.

If the Z value is more than 120, it represents marine limestone; otherwise, it depicts freshwater limestone.

The B contents of the Lower Ordovician vary between 1.25 and 35.20 μg/g with a mean of 12.46 μg/g. In particular, the B contents of the Tongzi Formation range from 3.44 μg/g to 35.20 μg/g with a mean of 16.51 μg/g, and those of the Honghuayuan Formation range from 1.25 μg/g to 13.60 μg/g with a mean of 8.40

μg/g (Figure 8). Although the B contents of the samples are lower than those of the marine sediment, the B contents of the Tongzi Formation are higher than those of the Honghuayuan Formation. The B content of the sediment is correlated with that of the water. Moreover, the B content has a positive linear relationship with water salinity [30]. As such, the B content of the marine sediment is higher than that of the freshwater sediment. Specifically, the B content of the marine sediment mostly ranges from 80 μg/g to 125 μg/g [31].

The B/Ga ratios of the Lower Ordovician range from 5.63 to 20.21 with a mean of 8.97, which is greater than 5.0. In particular, the B/Ga ratios of the Tongzi and Honghuayuan Formations vary between 6.19 and 20.21 with a mean of 10.28 and between 5.63 and 9.78 with a mean of 7.65, respectively (Figure 8). The B/Ga mean ratio of the Tongzi Formation is higher than that of the Honghuayuan Formation. B is common in marine sediments, whereas Ga generally exists in freshwater sediments. Thus, the B/Ga ratio is high in marine sediments. Wang Yiyou *et al.* [32] consider that the B/Ga ratios of terrestrial sediments, marine sediments, and transitional facies sediments are generally less than 3.0 to 3.3, more than 4.5 to 5.0, and between the first two ranges, respectively.

The brachiopods and crinoids in the Lower Ordovician also indicate a marine environment.

6.3. Paleowater Depth

During the Early Ordovician, the water depth ranged from 10 m to 200 m and increased. The $\delta^{13}C_{PDB}$ values of the Tongzi Formation range from −1.60‰ to 0.50‰ with a mean of −0.70‰, and those of the Honghuayuan Formation range from −1.00‰ to 0.10‰ with a mean of −0.41‰ (Figure 8). The $\delta^{13}C_{PDB}$ values have a tendency to increase in the vertical context. The Sr/Ba ratios of the Lower Ordovician vary between 0.38 and 17.16 with a mean ratio of 4.93. The Sr/Ba ratios of the Tongzi Formation range from 0.38 to 17.16 with a mean ratio of 4.17, and those of the Honghuayuan Formation range from 0.70 to 16.01 with a mean of 5.70 (Figure 8). The mean ratio of the Honghuayuan Formation is higher than that of the Tongzi Formation. When fresh water mixes with sea water, Ba^{2+} in the fresh water and SO_4^{2-} in the sea water combine to form $BaSO_4$. Moreover, Sr^{2+} and SO_4^{2-} combine to form $SrSO_4$. Compared with that of $BaSO_4$, the solubility of $SrSO_4$ is higher; thus, the latter can migrate seaward. Furthermore, because the radius of Ba^{2+} is smaller than that of Sr^{2+}, the ion electric potential of Ba^{2+} is small, and it can be easily absorbed by clay minerals, gels, and organic materials. The Sr content from land to sea has a tendency to increase, whereas the Ba content may decrease [33] [34] [35] [36] [37]. The abundance of crinoids demonstrates that water depth might be great. Penecontemporaneous dolomite signifies a shallower water depth.

6.4. Paleoxygenation Facies

The sedimentary environment during the Early Ordovician was generally oxygen-deficient. Nonetheless, the reducibility of the sedimentary environment was

enhanced from the sedimentary period of the Tongzi Formation to that of the Honghuayuan Formation. The V/(V + Ni) ratios of the Lower Ordovician vary between 0.51 and 0.83 with a mean of 0.68. In particular, the V/(V + Ni) ratios of the Tongzi Formation range from 0.59 to 0.83 with a mean of 0.71, and those of the Honghuayuan Formation range from 0.51 to 0.79 with a mean of 0.65 (Figure 8). Hatch *et al.* [38] investigate the Upper Pennsylvanian black shale in Kansas, North America and conclude that V/(V + Ni) ratios larger than 0.89 indicate a reductive environment. Similarly, V/(V + Ni) ratios ranging from 0.54 to 0.82 indicate a reductive environment in which the water column stratification is not obvious. However, V/(V + Ni) ratios smaller than 0.46 indicate an oxygen-deficient environment in which stratification is weak. The U/Th ratios of the Lower Ordovician vary between 0.39 and 2.93 with a mean of 1.07. In particular, the U/Th ratios of the Tongzi Formation range from 0.39 to 2.93 with a mean of 1.10, and those of the Honghuayuan Formation range from 0.51 to 2.10 with a mean of 1.04 (Figure 8). The V/Cr ratios of the Lower Ordovician are between 0.96 and 3.65 with a mean ratio of 1.50. For the Tongzi and Honghuayuan Formations, the V/Cr ratios vary between 0.96 and 2.23 with a mean of 1.41 and between 0.99 and 3.65 with a mean ratio of 1.59, respectively (Figure 8). The Ni/Co ratios of the Lower Ordovician range from 0.12 to 1.43 with a mean of 0.60. The Ni/Co ratios of the Tongzi and Honghuayuan Formations range from 0.31 to 1.43 with a mean of 0.71 and from 0.12 to 0.67 with a mean of 0.49, respectively (Figure 8). The U/Th, V/Cr, and Ni/Co ratios are reliable discriminant indexes for identifying an oxidative environment from a reductive one [39]. In a reductive environment, the U/Th, V/Cr, and Ni/Co ratios are greater than 1.125, 4.125, and 7, respectively. In an oxygen-deficient environment, the U/Th, V/Cr, and Ni/Co ratios vary between 0.175 and 1.125, between 2.1 and 4.125, and between 5 and 7, respectively. In an oxidative environment, the U/Th, V/Cr, and Ni/Co ratios are less than 0.175, 2, and 5 respectively. Yan Jiaxin *et al.* [40], on the basis of their research into the Qixia Formation in Shuibuya (Hubei), and Shi Chunhua *et al.* [41], on the basis of their work on the Qixia Formation in Laibin (Guangxi), point out that V/(V + Ni) and U/Th ratios can be used to judge the redox conditions of the paleoenvironment and that the reliability of V/Cr and Ni/Co ratios is questionable. The fact that the V/Cr and Ni/Co ratios of the samples in the present work correspond to an oxidative environment indicates that such ratios require further research, with regard to their use in determining the redox conditions of the ancient environment.

The $(Ce/La)_N$ ratios of the Lower Ordovician range from 0.77 to 0.98 with a mean of 0.85. For the Tongzi and Honghuayuan Formations, the $(Ce/La)_N$ ratios vary between 0.77 and 0.98 with a mean of 0.84 and between 0.81 and 0.91 with a mean of 0.86, respectively (Figure 6). The $(Ce/La)_N$ mean ratio of the Tongzi Formation is lower than that of the Honghuayuan Formation, thus indicating a reducibility enhancement. Bai Daoyuan *et al.* [42] assert that the $(Ce/La)_N$ ratio denotes an oxidative, an oxygen-deficient, and a reductive environment when it is less than 1.5, when it ranges from 1.5 to 1.8, and when it is more than 2.0, re-

spectively.

The Ce/Ce* ratios of the Lower Ordovician vary between 0.83 and 0.96 with a mean of 0.89. The Ce/Ce* ratios of the Tongzi and Honghuayuan Formations vary between 0.83 and 0.96 with a mean of 0.88 and between 0.88 and 0.96 with a mean of 0.91, respectively (Figure 6). The Ce/Ce* ratios of the Honghuayuan Formation are higher than those of the Tongzi Formation, thus indicating that the oxidability of the sedimentary environment might abate. Ce/Ce* ratios that are greater than 1 indicate positive anomalies, which reflect a reductive environment. By contrast, Ce/Ce* ratios that are less than 0.95 indicate negative anomalies, which reflect an oxidative environment.

The Eu/Eu* ratios of the Lower Ordovician range from 0.85 to 1.17 with a mean of 0.93, which indicates a weak oxidative environment. In particular, the Eu/Eu* ratios of the Tongzi Formation range from 0.87 to 0.99 with a mean of 0.92, and those of the Honghuayuan Formation range from 0.85 to 1.17 with a mean of 0.95 (Figure 6). Several samples have positive Eu anomalies, which may be related to transgression. This process forces some of the bottom water to evolve from an oxidative environment to a reductive one. When the Eu/Eu* ratio is greater than 1, Eu generally shows a positive anomaly, which indicates a reductive environment; otherwise, it shows a negative anomaly, which indicates an oxidative environment.

The Ce_{anom} values of the Lower Ordovician vary between −0.072 and 0.005 with a mean of −0.039. For the Tongzi and Honghuayuan Formations, the Ce_{anom} values vary between −0.072 and 0.005 with a mean of −0.044 and between −0.054 and −0.014 with a mean of –0.034, respectively (Figure 6). Given that the Ce_{anom} values of the Honghuayuan Formation are higher than those of the Tongzi Formation, the oxidability of the sedimentary environment weakened. Ce^{3+} is the main existence form of Ce in seawater and sediment. If the water has an oxidative environment, then Ce^{3+} is easily converted into Ce^{4+}, thus producing precipitation and displaying Ce negative anomaly [43]. Elderfield and Greaves [44] use Ce_{anom} to reflect the enrichment and loss of Ce and the redox conditions of the environment.

$$Ce_{anom} = \log_{10}\left[3Ce_n/\left(2La_n + Nd_n\right)\right]$$ (n representing north American shale standardization)

When Ce_{anom} is greater than −0.1, Ce increases and indicates a reductive environment. Contrarily, when Ce_{anom} is less than −0.1, Ce decreases and indicates an oxidative environment.

7. Conclusion

As indicated by the combination of its petrologic and geochemical characteristics, the lower part of the Tongzi Formation might have been formed from an evaporite platform into a restricted one, where the climate was dry, the water depth was shallow, and the oxygen was deficient. The upper part of this formation was assumed to be deposited in an open platform, which featured a humid climate and increased water depth and reducibility. During the sedimentary pe-

riod of the Honghuayuan Formation, the water energy further increased, the climate became humid, the water depth was great, and the reducibility increased. The sedimentary environment, which originally comprised littoral facies that slowly developed into an open platform and into a platform marginal bank, gradually evolved into a platform marginal reef. Petrologic features are the foundation. Compared with them, some geochemical indicators may be more precisely. Though influenced by provenance, diagenesis and so on, some indicators are more reliable and are suggested to be emphasized.

Acknowledgements

References

[1] Li, J.C., Ma, Y.S. and Zhang, D.J. (1998) Some Very Important Science and Technology Problems in the Marine Oil and Gas Explorations of China. *Petroleum Exploration and Development*, **24**, 1-2.

[2] Tian, H.Q. (1998) Study and Mapping of Quantitative Lithofacies Palaeogeography of the Cambrian in South China. Petroleum University Press, Dongying.

[3] Tian, H.Q., Wo, Y.J., Zheng, L., Shong, L.H. and Wan, Z.M. (2002) Thought on the Oil and Natural Gas Exploration Direction of Mesozoic-Paleozoic Strata in Southern China. *Southern China Oil and Gas*, **13**, 618.

[4] Tian, H.Q., Guo, T.L., Song, L.H. and Yang, Z.Q. (2004) The Lower Marine Combination in North Western Guizhou Province: An Noticeable Exploration Area. *Southern China Oil and Gas*, **17**, 1-5.

[5] Tian, H.Q., Guo, T.L., Hu, D.F., Tang, L.J., Wo, Y.J., Song, L.H., *et al.* (2006) Marine Lower Assemblage and Exploration Prospect of Central Guizhou Uplift and Its Adjacent Areas. *Journal of Palaeogeography*, **8**, 509-518.

[6] Feng, Z.Z., Peng, Y.M., Jin, Z.K., Jiang, P.L., Bao, Z.D., Luo, Z., *et al.* (2001) Lithofacies Palaeogeography of the Cambrian in South China. *Journal of Palaeogeography*, **3**, 1-14.

[7] Feng, Z.Z., Peng, Y.M., Jin, Z.K., Jiang, P.L., Bao, Z.D., Luo, Z., *et al.* (2001b) Lithofacies Palaeogeography of the Early Ordovician in South China. *Journal of Palaeogeography*, **3**, 11-22.

[8] Feng, Z.Z., Peng, Y.M., Jin, Z.K., Jiang, P.L., Bao, Z.D., Luo, Z., *et al.* (2001c) Lithofacies Palaeogeography of the Middle and Late Ordovician in South China. *Journal of Palaeogeography*, **3**, 10-24.

[9] Deng, X., Yang, K.G., Liu, Y.L. and She, Z.B. (2010) Characteristics and Tectonic Evolution of Qianzhong Uplift. *Earth Science Frontiers*, **17**, 79-89.

[10] Yin, G.Z. (1980) New Material of Ordovician Trilobites from Northern Guizhou. *Acta Palaeontologica Sinica*, **19**, 23-27.

[11] Yin, G.Z. (1986) Ordovician Trilobite Succession in Guizhou, China. *Geology of Guizhou*, **3**, 410-424.

[12] Yue, S.X. (1959) Some New Coral Species from the Ordovician of Kueichow Province, Southwestern China. *Acta Scientiarum Naturalium Universitatis Pekinensis*, **5**, 395-414.

[13] Zhen, Y.Y., Percival, I.G. and Liu, J.B. (2006) Rhipidognathid Conodonts from the Early Ordovician Honghuayuan Formation of Guizhou, South China. *Palaeoworld*, **15**, 194-210. https://doi.org/10.1016/j.palwor.2006.07.004

[14] Wang, G. (1986) A Discussion on Chronostratigraphy of Ordovician in Guizhou Province. *Geology of Guizhou*, **3**, 385-409.

[15] Mei, M.X. (1989) The Features of Lithofacies Paleogeography of Tongzi Age in Guizhou Province and Its Adjacent Areas. *Geology of Guizhou*, **6**, 217-226.

[16] Mei, M.X. and Zeng, Y. (1989) Ordovician Honghuayuanian Sedimentary Facies and Palaeogeography in Guizhou and Its Adjacent Area. *Sedimentary Geology and Tethyan Geology*, **8**, 15-25.

[17] Ma, Y.S., Chen, H.D. and Wang, G.L. (2009a) Sequence Stratigraphy and Palaeogeography in Southern China. Science Press, Beijing, 1-603.

[18] Ma, Y.S., Chen, H.D. and Wang, G.L. (2009b) Tectonic Sequence Lithofacies Paleogeographic Atlas in Southern China. Science Press, Beijing, 1-301.

[19] Duan, T.Z., Zeng, Y.F. and Gao, Z.Z. (1988) Analysis of Tectonic Evolution of Paleocontinental Margin in South China Based on Sedimentary History. *Oil and Gas Geology*, **9**, 410-420.

[20] Zheng, H.R. and Hu, Z.Q. (2010) Pre-Mesozoic Tectonic Lithofacies Paleogeographic Atlas of China. Geological Publishing House, Beijing, 71-74.

[21] Wang, X.F., Chen, X.H., Wang, C.S. and Li, Z.H. (2004) Ordovician to the Lowest Silurian Chronostratigraphic Subdivision in China. *Journal of Stratigraphy*, **28**, 1-17.

[22] Regional Geological Team of Geological Survey, Guizhou Province (1965) Geological Map of Duyun (G-48-XVIII). Springer Publishing, New York.

[23] Yan, J.X., Wu, M., Li, F.L. and Fang, N.Q. (1998) Geochemistry of Sedimentation and Diagenesis in Qixia Formation (Early Permian) of Badong, Hubei Province. *Acta Sedimentologica Sinica*, **16**, 78-83.

[24] Kaufman, A.J., Jacobsen, S.B. and Knoll, A.H. (1993) The Vendian Record of Sr and C Isotopic Variations in Seawater: Implications for Tectonics and Paleoclimate. *Earth and Planetary Science Letters*, **120**, 409-430.

[25] Derry, L.A., Brasier, M.D., Corfield, R.M., Rozanov, A.Y. and Zhuravlev, A.Y. (1994) Sr and C Isotopes in Lower Cambrian Carbonates from the Siberian Craton: A Paleoenvironmental Record during the Cambrian Explosion. *Earth and Planetary Science Letters*, **120**, 678-681. https://doi.org/10.1016/0012-821x(94)90178-3

[26] Shao, L.Y., He, H., Peng, S.P. and Li, R.J. (2002) Types and Origin of Dolostones of the Cambrian and Ordovician of Bachu Uplift Area in Tarim Basin. *Journal of Palaeogeography*, **4**, 19-30.

[27] Ni, S.Q., Hou, Q.L., Wang, A.J. and Ju, Y.W. (2010) Geochemical Characteristics of Carbonate Rocks and Its Geological Implications-Taking the Lower Palaeozoic Carbonate Rock of Beijing Area as an Example. *Acta Geologica Sinica*, **84**, 1510-1516.

[28] Epstein, S. and Mayeda, T. (1953) Variation of O^{18} Content of Waters from Natural Sources. *Geochimica et Cosmochimica Acta*, **4**, 213-224. https://doi.org/10.1016/0016-7037(53)90051-9

[29] Keith, M.L. and Weber, J.N. (1964) Carbon and Oxygen Isotopic Composition of Selected Limestones and Fossils. *Geochimica et Cosmochimica Acta*, **28**, 1787-1816. https://doi.org/10.1016/0016-7037(64)90022-5

[30] Couch, E.L. (1971) Calculation of Paleosalinities from Boron and Clay Mineral Data. *AAPG Bulletin*, **55**, 1829-1837.

[31] Wang, Z.H. and Jiao, Y.Q. (2004) Characteristics of Element Geochemistry of Shuixigou Group in North-Eastern Tu-Ha Basin. *Coal Geology and Exploration*, **32**, 1-4.

[32] Wang, Y.Y., Guo, W.Y. and Zhang, G.D. (1979) Application of Some Geochemical Indicators in Determing of Sedimentary Environment of Funing Group, Jinhu Depression, Kiangsu Province. *Journal of Tongji University*, 51-69.

[33] Huang, S.J., Wu, S.J., Sun, Z.L., Pei, C.R. and Hu, Z.W. (2005) Seawater Strontium Isotopes and Paleooceanic Events over the Past 260 Ma. *Earth Science Frontiers*, **12**, 133-141.

[34] Wang, K.M. and Luo, S.S. (2009) Strontium Isotope and Trace Element Characteristics of Marine Carbonate and Sea Level Fluctuation. *Marine Geology and Quaternary Geology*, **29**, 51-58. https://doi.org/10.3724/SP.J.1140.2010.06051

[35] Wang, K.M. and Luo, S.S. (2009b) Geochemical Characteristics and Environmental Significance of Gaoyuzhuang and Yangzhuang Formations in Yanshan Region. *Bulletin of Mineralogy, Petrology and Geochemistry*, **28**, 356-364.

[36] Veizer, J. and Demovic, R. (1974) Strontium as a Tool for Facies Analysis. *Sedimentary Petrology*, **44**, 93-115.

[37] Liu, Y.J., Cao, L.M. and Li, Z.L. (1984) Element Geochemistry. Science Press, Beijing, 360-372.

[38] Hatch, J.R. and Leventhal, J.S. (1992) Relationship between Inferred Redox Potential of the Depositional Environment and Geochemistry of the Upper Pennsylvanian (Missourian) Stark Shale Member of the Dennis Limestone, Wabaunsee County, Kansas, USA. *Chemical Geology*, **99**, 65-82. https://doi.org/10.1016/0009-2541(92)90031-Y

[39] Jones, B. and Manning, A.C. (1994) Comparison of Geochemical Indices Used for the Interpretation of Palaeoredox Conditions in Ancient Mudstones. *Chemical Geology*, **111**, 111-129. https://doi.org/10.1016/0009-2541(94)90085-X

[40] Yan, J.X., Xu, S.P. and Li, F.L. (1998b) Geochemistry of the Anaerobic Sedimentary Environments of the Qixia Formation in Badong, Hubei. *Sedimentary Facies and Palaeogeography*, **18**, 27-32

[41] Shi, C.H., Huang, Q. and Yan, J.X. (2001) Geochemistry of the Anaerobic Sedimentary Environments of Qixia Formation in Laibin, Guangxi. *Sedimentary Geology and Tethyan Geology*, **21**, 72-77.

[42] Bai, D.Y., Zhou, L., Wang, X.H. and Zhang, X.Y. (2007) Geochemistry of Nanhua-Cambrian Sandstones in Southeastern Hunan, and Its Constraints on Neoproterozoic-Early Paleozoic Tectonic Setting of South China. *Acta Geologica Sinica*, **81**, 755-771.

[43] Wang, Z.G., Yu, X.Y. and Zhao, Z.H. (1989) Geochemistry of Rare Earth Elements. Science Press, Beijing, 90-93.

[44] Elderfield, H. and Greaves, M.J. (1982) The Rare Earth Elements in Seawater. *Nature*, **296**, 214-219. https://doi.org/10.1038/296214a0

❖ Scientific Research Publishing ❖